IEEE Access
Multidisciplinary | Rapid Review | Open Access Journal

Received March 16, 2018, accepted May 8, 2018, date of publication May 23, 2018, date of current version June 29, 2018.

Digital Object Identifier 10.1109/ACCESS.2018.2839766

Human Daily and Sport Activity Recognition Using a Wearable Inertial Sensor Network

YU-LIANG HSU[1], (Member, IEEE), SHIH-CHIN YANG[2], (Member, IEEE), HSING-CHENG CHANG[1], AND HUNG-CHE LAI[1]

[1]Department of Automatic Control Engineering, Feng Chia University, Taichung 40724, Taiwan
[2]Department of Mechanical Engineering, National Taiwan University, Taipei 10617, Taiwan

Corresponding author: Yu-Liang Hsu (hsuyl@fcu.edu.tw)

This work was supported by the Ministry of Science and Technology of the Republic of China, Taiwan, under Grants MOST 106-2221-E-035-004 and MOST 106-3011-E-006-002.

ABSTRACT This paper presents a wearable inertial sensor network and its associated activity recognition algorithm for accurately recognizing human daily and sport activities. The proposed wearable inertial sensor network is composed of two wearable inertial sensing devices, which comprise a microcontroller, a triaxial accelerometer, a triaxial gyroscope, an RF wireless transmission module, and a power supply circuit. The activity recognition algorithm, consisting of procedures of motion signal acquisition, signal preprocessing, dynamic human motion detection, signal normalization, feature extraction, feature normalization, feature reduction, and activity recognition, has been developed to recognize human daily and sport activities by using accelerations and angular velocities. In order to reduce the computational complexity and improve the recognition rate simultaneously, we have utilized the nonparametric weighted feature extraction algorithm with the principal component analysis method for reducing the feature dimensions of inertial signals. All 23 participants wore the wearable sensor network on their wrist and ankle to execute 10 common domestic activities in human daily lives and 11 sport activities in a laboratory environment, and their activity recordings were collected to validate the effectiveness of the proposed wearable inertial sensor network and activity recognition algorithm. Experimental results showed that our approach could achieve recognition rates for the 10 common domestic activities of 98.23% and 11 sport activities of 99.55% by the 10-fold cross-validation strategy, which have successfully validated the effectiveness of the proposed wearable inertial sensor network and its activity recognition algorithm.

INDEX TERMS Wearable inertial sensing device, body sensor network, daily activity recognition, sport activity recognition, nonparametric weighted feature extraction, support vector machine.

I. INTRODUCTION

With rapid advancements in computer and miniaturization technologies, human activity recognition systems based on wearable and low-cost sensors have become an important part of our daily lives and are widely used in numerous applications such as health management, medical monitoring, human computer interaction, robotics, surveillance, sport science, rehabilitation, remote control, and so on [1]–[11]. For existing activity recognition systems, a wearable device embedded with inertial sensors has been developed to detect human activities for recognizing daily and sport activities. A salient advantage of wearable devices embedded with inertial sensors for activity monitoring and recognition is that they can be operated without any external ambient-based sensors (such as radar, camera, or infrared sensors) or limitation in working conditions [12]–[17].

Recently, many researchers have focused on developing effective human daily activity recognition systems through combining various feature reduction methods with machine learning classifiers to measurements collected from wearable devices. To name a few, Xiao and Lu [18] presented the kernel discriminant analysis (KDA) based extreme learning machine (ELM) for recognizing daily human physical activities using an accelerometer placed on the subject's thigh. Altun *et al.* [19] used the principal component analysis (PCA) method to reduce the input features from 1170 to 30 to represent a motion signal sample, which were captured from the human activity signals measured by the MTx trackers

mounted on the user's wrist, knee, and chest in a laboratory environment. Subsequently, the 30 PCA-based features were treated as the input features for the Bayesian decision making classifier. Yang *et al.* [20] combined the common PCA (CPCA) with the support vector clustering (SVC) algorithm to develop the feature subset selection (FSS) algorithm for the 24 features extracted from the static and dynamic activities, which were collected in a laboratory environment. The 8 common domestic activities composed of standing, sitting, walking, running, vacuuming, scrubbing, brushing teeth, and working at a computer were recognized by the FSS combined with the feedforward neural network (FNN). Khan *et al.* [21] utilized the KDA-based support vector machines (SVMs) to recognize 15 human activities in a laboratory environment using the measurements of the accelerometer, pressure sensor, and microphone. Chen *et al.* [22] combined the dynamic linear discriminant analysis (LDA) with the fuzzy basis function (FBF) classifiers for classifying 8 human daily activities in a laboratory environment with satisfactory recognition accuracy. From the abovementioned literature review, the most feature reduction methods used to combine with the machine learning classifiers are the unsupervised feature extraction methods (PCA and CPCA) and discriminant analysis feature extraction methods (KDA and LDA). However, there are some limitations using the unsupervised and discriminant analysis feature extraction methods to deal with recognition problems, for example, the eigenvectors extracted by PCA are not robust to variations in the durations of subjects' activities [23] and only most $C-1$ (number of classes minus one) features can be extracted by discriminant analysis feature extraction methods [24], [25]. Hence, the nonparametric feature extraction methods are developed for dealing with recognition tasks [24], [25].

In addition, in recent years wearable inertial sensing devices have become a popular solution for sport activity recognition applications, since they are small in size, light weight, low cost, and low power consumption. Ermes *et al.* [5] utilized the hybrid classifier combining the tree structure and the artificial neural network (ANN) to recognize 9 daily and sport activities. The accuracy for categorizing 9 daily and sport activities using both supervised and unsupervised data was 89% by the 12-fold leave-one-subject-out cross-validation. Margarito *et al.* [6] compared the recognition performance of the template-matching and statistical-learning classifiers for recognizing 8 common sport activities using a triaxial accelerometer wore on users' wrist.

Based on the abovementioned literature review, a wearable inertial sensor network combined a nonparametric feature extraction method with a machine learning classifier was developed to obtain better accuracy for daily and sport activity recognition. The proposed wearable inertial sensor network is placed on users' wrist and ankle for measuring motion signals while executing daily and sport activities without any external ambient-based sensors. When users wear the wearable network on their wrist and ankle, daily and sport activities can be recognized by an activity recognition algorithm which is composed of the procedures of motion signal acquisition, signal preprocessing, dynamic human motion detection, signal normalization, feature extraction, feature normalization, feature reduction, and activity recognition. In order to reduce input feature dimensions and further improve the recognition performance, we have utilized a feature reduction method, which combines the nonparametric weighted feature extraction (NWFE) [24] with the principal component analysis (PCA) [33], to extract the characteristic features from a total of 252 normalized time- and frequency-domain features. Finally, we use a least squares support vector machine (LS-SVM) recognizer to classify 10 human daily activities and 11 sport activities. The contribution of this paper is to develop a low cost wearable inertial sensor network and its activity recognition algorithm which utilizes the NWFE-PCA-based feature reduction method with a machine learning classifier (LS-SVM) for obtaining better accuracy for human daily and sport activity recognition, which can be used to provide an effective tool for human daily and sport activity recognition tasks.

The rest of this paper is organized as follows. In Section II, the demographics and participant characteristics, and hardware architecture of the proposed wearable inertial sensor network are described in detail. The activity recognition algorithm, composed of motion signal acquisition, signal preprocessing, dynamic human motion detection, signal normalization, feature extraction, feature normalization, NWFE-PCA-based feature reduction, and LS-SVM recognizer, is described in Section III. Sections IV presents the experimental results and discussions. Finally, the conclusions are given in Section V.

II. EXPERIMENTAL SETUP

A. PARTICIPANTS

In this study, we collected human motion signals for the daily activity recognition experiment from 13 healthy subjects (3 females, 10 males; age $= 22.9 \pm 1.6$ years; height $= 169.5 \pm 6.2$ cm; mass $= 66.9 \pm 13.2$ kg). In addition, for the sport activity recognition experiment, the sport motion signals were collected from all 10 participants (3 females, 7 males; age $= 21.4 \pm 0.8$ years; height $= 168.7 \pm 7.2$ cm; mass $= 60.1 \pm 12.7$ kg) chosen from the 13 healthy subjects. Each participant was asked to execute 10 daily activities or 11 sport activities with each activity executed 10 times. Therefore, the recognition performances of the proposed wearable inertial sensor network and its associated activity recognition algorithm were validated using a total number of 1300 ($= 13 \times 10 \times 10$) and 1100 ($= 10 \times 11 \times 10$) data of 10 daily activities and 11 sport activities, respectively. All participants were instructed to perform each daily and sport activity for 30 s and 15 s, respectively.

The demographics of the participants for the daily and sport activity recognition experiments are summarized in Table 1. The experimental protocol used in this paper

TABLE 1. Participant characteristics for daily and sport activity recognition experiments.

Parameters	Daily Activity	Sport Activity
Men/Women (n)	10/3	7/3
Age (years)	22.9 ± 1.6	21.4 ± 0.8
Height (cm)	169.5 ± 6.2	168.7 ± 7.2
Weight (kg)	66.9 ± 13.2	60.1 ± 12.7
BMI (kg/m^2)	23.1 ± 3.6	21.0 ± 3.2

was approved by Institutional Review Board (IRB) of the National Cheng Kung University Hospital. All subjects were required to provide written informed consent before study participation.

B. APPARATUS

In this paper, we have implemented a wearable inertial sensor network composed of two inertial sensing devices which are worn on the subjects' dominant side (one on the wrist and one on the lateral ankle) to collect motion signals of human daily and sport activities shown in Fig. 1. The architecture of the wearable inertial sensing device consists of a microcontroller (Arduino Pro Mini), a six-axis inertial sensor module (MPU-6050), an RF wireless transmission module (nRF24L01), and a power supply circuit. The schematic diagram of the wearable inertial sensor network is shown in Fig. 2. The microcontroller embedded in the inertial

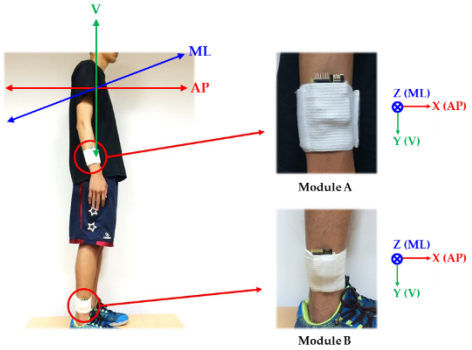

FIGURE 1. Wearable inertial sensor network mounted on subject's wrist and ankle.

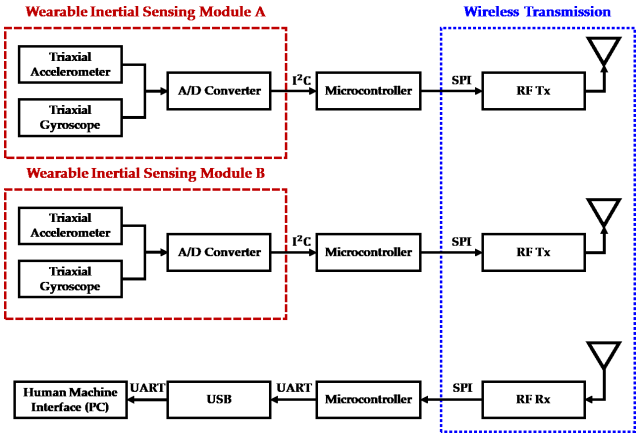

FIGURE 2. Schematic diagram of the wearable inertial sensor network.

sensing device was implemented using an Arduino Pro Mini device with an ATmega328 core operating at a frequency of 16 MHz and 32 Kbytes of flash memory. The microcontroller collected the digital human motion signals measured from the six-axis inertial sensor module through an I^2 C interface and then transmitted the signals to a personal computer (PC) via the RF wireless transceiver (nRF24L01) through an SPI interface. The six-axis inertial sensor module comprises a triaxial accelerometer, a triaxial gyroscope, and 16 bit analog to digital converters (ADCs), which is utilized to simultaneously collect the accelerations and angular velocities generated from human daily and sport activities in a three-dimensional space and output the digital human motion signals. The accelerometer can detect the gravitational and X- (anteroposterior, AP), Y- (vertical, V), and Z- (mediolateral, ML) axis motion accelerations of the inertial sensing devices mounted on subjects' wrist and ankle during executing daily and sport activities, and has a full scale of ±2, ±4, ±8, and ±16 g. The gyroscope can measure the angular velocities of hand and foot motions, and possesses a user selectable full scale of ±250, ±500, ±1000, and ±2000 °/s. In performing the daily and sport activities, the range and sensitivity of the accelerometer were configured as ±16 g and 2048 LSB/g, while which of the gyroscope were set as ±2000 °/s and 16.4 LSB/°/s. The output signals of the accelerometer and gyroscope were sampled at a frequency of 100 Hz. The power supply circuit provides the power consumption for the wearable inertial sensing device, which is composed of a Li-ion battery, a Li-ion battery charging module, and regulators. The wearable inertial sensing device shown in Fig. 3 (including the circuit board, RF wireless module, and battery) was measured 56 mm × 37 mm × 15 mm with weight of 16 grams and was powered by a 3.7 V polymer Li-ion battery with a nominal capacity of 450 mAh.

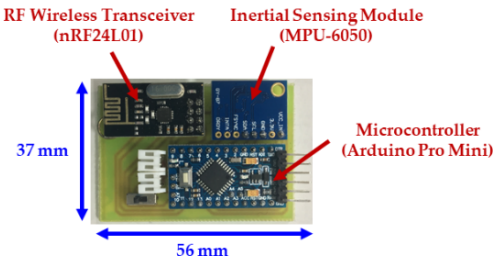

FIGURE 3. The proposed wearable inertial sensing device.

III. ACTIVITY RECOGNITION ALGORITHM

In this paper, we have implemented an activity recognition algorithm to recognize human daily and sport activities by using the accelerations and angular velocity signals. The activity recognition algorithm is composed of the following procedures: 1) motion signal acquisition, 2) signal preprocessing, 3) dynamic human motion detection, 4) signal normalization, 5) feature extraction, 6) feature normalization,

7) NWFE-PCA-based feature reduction, and 8) LS-SVM recognizer. At the beginning of the procedures, the human motion signals measured from the accelerometer and gyroscope are collected by the microcontroller embedded in the wearable inertial sensing devices and then transmitted to the PC-based human machine interface via the RF wireless transmission module. Second, a calibration process, a designed lowpass filter, and a designed highpass filter are utilized to eliminate the sensitivity and offset errors of the sensors, users' unconscious trembles, and gravitational acceleration, respectively, in the signal preprocessing procedure. Third, an adaptive magnitude threshold method for detecting the dynamic human motion based on the magnitude thresholds of the signal vector magnitudes of the filtered accelerations and angular velocities, respectively. Fourth, we normalize each dynamic human motion signal into equal size via the signal normalization procedure. Fifth, 21 time- and frequency-domain motion features are extracted from the triaxial accelerations and angular velocities generated from the hand and foot motions for recognizing 10 human daily activities and 11 sport activities. Sixth, the min-max normalization method is used to normalize each feature for eliminating the effects of the variation in the range of values of the extracted features. Subsequently, we reduce the dimensions of the normalized features by using the NWFE+PCA method. Finally, the LS-SVM recognizer is utilized to recognize human daily or sport activities using the dimension-reduced features as the recognizer inputs. The block diagram of the proposed activity recognition algorithm is shown in Fig. 4. We now introduce the detailed procedures of the proposed activity recognition algorithm.

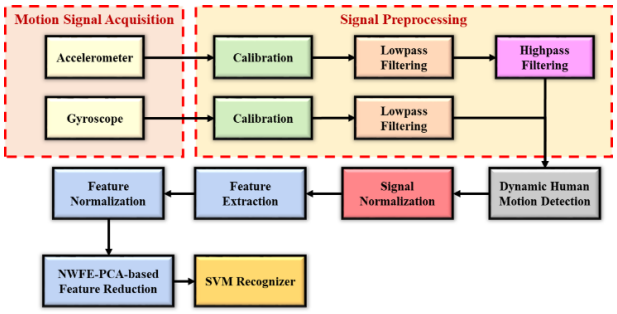

FIGURE 4. The proposed activity recognition algorithm.

A. SIGNAL PREPROCESSING

Since the measured accelerations and angular velocities are always contaminated not only by the sensitivity and offset errors of the sensors but also with users' unconscious trembles, signal preprocessing composed of calibration and lowpass filtering is a required procedure after motion signal acquisition [8], [12]. In addition, we have to remove the gravitational acceleration included in the measured accelerations to obtain the motion accelerations generated from the human daily or sport activities. In this paper, we first calibrate the accelerometer and gyroscope, and then filter the high frequency noise of the acceleration and angular velocity signals via a digital lowpass filter. Finally, the gravitational acceleration is filtered from the lowpass-filtered accelerations via a digital highpass filter.

1) CALIBRATION AND LOWPASS FILTERING

In this paper, we utilize the calibration method proposed in [7] and [26] to calculate the scale factor (S) and offset (O) of each axis of the accelerometer and gyroscope, respectively, which are used to reduce sensitivity and offset errors from the raw acceleration and angular velocity signals. Subsequently, we further reduce the high frequency noise of the calibrated accelerations or angular velocities by using a moving average filter.

$$c_l[n] = \frac{1}{N}\sum_{i=1}^{N} c_c[n-i], \tag{1}$$

where c_c is the calibrated triaxial accelerations (a_{cx}, a_{cy}, and a_{cz}) or triaxial angular velocities (ω_{cx}, ω_{cy}, and ω_{cz}), while c_l is the lowpass-filtered triaxial accelerations (a_{lx}, a_{ly}, and a_{lz}) or triaxial angular velocities (ω_{lx}, ω_{ly}, and ω_{lz}). N is the number of points in the average filter. In this paper, according to our empirical tests, we set $N = 15$ and 5 for the motion signals generated from the hand and foot movements, respectively.

2) HIGHPASS FILTERING

After lowpass-filtering of the accelerations, a highpass filter should be utilized to remove the gravitational acceleration [27], [28]. In this paper, we utilize a three-order highpass elliptic filter with cut-off frequency of 0.005 Hz to remove the gravitational acceleration from the lowpass-filtered acceleration (a_{lx}, a_{ly}, and a_{lz}) to obtain triaxial motion accelerations (a_{hx}, a_{hy}, and a_{hz}) caused by hand and foot movements.

B. DYNAMIC HUMAN MOTION DETECTION

An adaptive magnitude threshold method has been developed to automatically detect human motion of each daily and sport activities from the filtered accelerations and angular velocities generated from hand and foot motions. The proposed adaptive magnitude threshold method is composed of the steps described as follows.

Step 1 (Calculation of Signal Vector Magnitudes): We use the signal vector magnitudes of the filtered accelerations and angular velocities to represent a measure of the degree of motion intensity of daily and sport activity motions [7], [26].

Step 2 (Calculation of Adaptive Magnitudes of Signal Vector Magnitudes): We calculate the adaptive magnitudes of the signal vector magnitudes of the filtered accelerations ($M_a(k)$) and angular velocities ($M_\omega(k)$), named TH_a and TH_ω, by setting the multiples of the mean values of $M_a(k)$ and $M_\omega(k)$ at the beginning of an activity (motion), denoted as t_i.

$$TH_a = K_a \times \underset{k}{mean}\,(M_a(k)), \tag{2}$$

$$TH_\omega = K_\omega \times \underset{k}{mean}(M_\omega(k)), \tag{3}$$

where k is the time steps in the interval of t_i, and K_a and K_ω are empirical values according to our empirical tests. In this paper, the K_a and K_ω are set as 1.02 and 7.8 for detecting the dynamic human motion interval, respectively.

Step 3 (Finding Start Points of an Activity Motion): Once we obtain the adaptive magnitude thresholds of the signal vector magnitudes of the filtered accelerations and angular velocities, the start point of the dynamic human motion interval of the activity motion can be determined by selecting the time steps whose magnitudes are higher than the thresholds. That is, the signal vector magnitudes of the filtered accelerations or angular velocities should be higher than the magnitude thresholds and maintain at least 20 time steps continuously to avoid the influence of users' unconscious trembles. Once the signal vector magnitudes of the filtered accelerations or angular velocities within the 20 time steps are all higher than the thresholds, the first time step point of the 20 time steps can be chosen as the candidates of the start point of a dynamic human motion interval within an activity motion. With the thresholds of the filtered accelerations and angular velocities, we can obtain the four candidates of the start point for the dynamic human motion interval, $t_{hand}^{a,start}$, $t_{hand}^{\omega,start}$, $t_{foot}^{a,start}$, and $t_{foot}^{\omega,start}$. We then determine the start point of the dynamic human motion interval of an activity motion by choosing the minimum value of the four candidates of the start point.

$$t_{motion}^{start} = min(t_{hand}^{a,start}, t_{hand}^{\omega,start}, t_{foot}^{a,start}, t_{foot}^{\omega,start}), \tag{4}$$

where t_{motion}^{start} is the start point of the dynamic human motion interval.

Step 4 (Finding end Points of an Activity Motion): Similarly, the end point of the dynamic human motion interval of the activity motion can be determined by selecting the time steps whose magnitudes are lower than the thresholds. Once the signal vector magnitudes of the filtered accelerations or angular velocities within the 20 time steps are all lower than the thresholds, the first time step point of the 20 time steps can be chosen as the candidates of the end point of a dynamic human motion interval within an activity motion. With the thresholds of the filtered accelerations and angular velocities, we can obtain the four candidates of the end point for the dynamic human motion interval, $t_{hand}^{a,end}$, $t_{hand}^{\omega,end}$, $t_{foot}^{a,end}$, and $t_{foot}^{\omega,end}$. We then determine the end point of the dynamic human motion interval of an activity motion by choosing the maximum value of the four candidates of the end point.

$$t_{motion}^{end} = max(t_{hand}^{a,end}, t_{hand}^{\omega,end}, t_{foot}^{a,end}, t_{foot}^{\omega,end}), \tag{5}$$

where t_{motion}^{end} is the end point of the dynamic human motion interval.

Once we can obtain the start and end points of the dynamic human motion interval (t_{motion}^{start} and t_{motion}^{end}), the static phase within the daily or sport activity motion can also be determined. The curves in Fig. 5 are filtered accelerations and angular velocities measured from the accelerometers and gyroscopes mounted on users' wrist and ankle directly. Fig. 5 is used to illustrate how to determine the dynamic human motion interval by using the proposed dynamic human motion detection method. The region with no color and the region with a grey color represent the dynamic and static intervals, respectively.

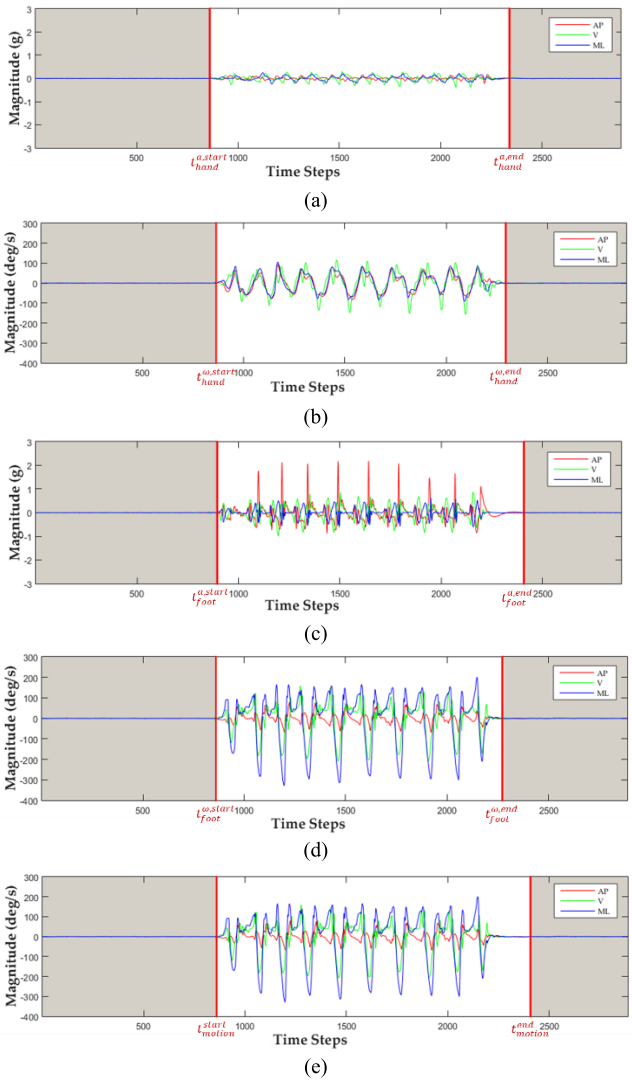

FIGURE 5. The partition of the dynamic human motion interval by using the proposed dynamic human motion detection method. (a) Detection of the $t_{hand}^{a,start}$ and $t_{hand}^{a,end}$ for the hand acceleration. (b) Detection of the $t_{hand}^{\omega,start}$ and $t_{hand}^{\omega,end}$ for the hand angular velocity. (c) Detection of the $t_{foot}^{a,start}$ and $t_{foot}^{a,end}$ for the foot acceleration. (d) Detection of the $t_{foot}^{\omega,start}$ and $t_{foot}^{\omega,end}$ for the foot angular velocity. (e) Partition of the human motion interval of the foot angular velocity into dynamic and static phases based on t_{motion}^{start} and t_{motion}^{end} simultaneously.

C. SIGNAL NORMALIZATION

Once the dynamic human motion interval is determined via the proposed dynamic human motion detection method, the size of the human motion signals of each human daily and sport motion between fast and slow users is inconsistence. Hence, after extracting the signals within the dynamic

human motion interval, we have to normalize each segmented dynamic human motion interval into the size of the signal with the longest length via interpolation.

D. FEATURE EXTRACTION

Once the normalized hand accelerations, hand angular velocities, foot accelerations, and foot angular velocities of each dynamic phase of each activity motion is obtained, the time- and frequency-domain motion features of each activity motion can be extracted from the X- (AP), Y- (V), and Z- (ML) axis normalized hand accelerations, hand angular velocities, foot accelerations, and foot angular velocities, respectively. The motion features including 1) mean, 2) mean absolute value, 3) harmonic mean, 4) maximum value, 5) minimum value, 6) range, 7) standard deviation, 8) variance, 9) interquartile range, 10) correlation coefficient, 11) skewness, 12) kurtosis, 13) mean absolute deviation, 14) root mean square, 15) simple squared integral, 16) slope sign change, 17) cumulative length, 18) zero crossing, 19) spectral entropy, 20) frequency energy, and 21) peak frequency are used for recognizing the human daily and sport motion patterns [4], [13], [17], [27], [29].

E. FEATURE NORMALIZATION

When the procedure of feature extraction is done, a total of 252 ($= 2 \times 2 \times 3 \times 21$) motion features are then generated. However, the variation in the range of values of the extracted features may influence the recognition results. Thus we map them in the new range $[f^n_{min}, f^n_{max}]$ by the min-max normalization method. The min-max normalization equation is shown as follows:

$$f^n(i) = \frac{f(i) - f_{min}(i)}{f_{max}(i) - f_{min}(i)} \left(f^n_{max} - f^n_{min}\right) + f^n_{min}, \tag{6}$$

where $f(i)$ is the ith original extracted motion feature, $f_{max}(i)$ and $f_{min}(i)$ are the maximum and minimum value among ith motion feature value extracted from the all subjects, respectively, and $f^n(i)$ is the ith normalized feature value. f^n_{min} and f^n_{max} are set to -1 and 1 in this study.

F. FEATURE REDUCTION

From the feature extraction and feature normalization procedures, the normalized feature vectors are high-dimensional vectors. However, redundant features not only decreases the performance of recognizers but also increases the computational complexity. Therefore, to reduce the dimensionality of the normalized feature vectors for constructing effective recognizers is the most important procedure for any recognition problems. In other words, feature reduction procedure can increase the recognition accuracy and reduce the computational complexity. In this paper, the nonparametric weighted feature extraction (NWFE) [24] combined with the principal component analysis (PCA) [33] is utilized for further selecting the appropriate features out of a total of 252 normalized features effectively and improve the recognition performance.

1) NONPARAMETRIC WEIGHTED FEATURE EXTRACTION

The goal of the NWFE is used to assign every sample with different weights and to define nonparametric between-class and within-class scatter matrices for finding a linear transformation which can maximize the nonparametric between-class scatter and minimize the nonparametric within-class scatter [24], [25]. In general, the discriminant analysis feature extraction is often utilized to reduce dimension of features in classification problems. The main disadvantage of the discriminant analysis feature extraction is that only most C–1 (number of classes minus one) features can be extracted. However, only using C–1 features is not sufficient for real measurements in classification problems [24]. That is, the discriminant analysis feature extraction has a poor performance on high-dimensional classification problems. In order to solve the abovementioned problems, NWFE is developed to assign different weights on every sample for calculating the weighted means and compute new nonparametric between-class and within-class scatter matrices for obtaining more than C–1 features to deal with high-dimensional classification problems.

At first, we calculate the nonparametric between-class scatter matrix ($\mathbf{S}_B^{NW}$) of NWFE in the original space $\mathbb{R}^m$ as follows:

$$\mathbf{S}_B^{NW} = \sum_{i=1}^{C} \sum_{\substack{j=1 \\ j \neq i}}^{C} \sum_{k=1}^{n_i} \frac{\lambda_k^{i,j}}{n_i} \left(x_k^i - M_j\left(x_k^i\right)\right)\left(x_k^i - M_j\left(x_k^i\right)\right)^T, \tag{7}$$

where x_k^i represents the kth sample in class i, n_i is the number of sample of class i, C is the number of classes, and the scatter matrix weight ($\lambda_k^{i,j}$) is defined as follows:

$$\lambda_k^{i,j} = \frac{dist\left(x_k^i, M_j\left(x_k^i\right)\right)^{-1}}{\sum_{h=1}^{n_i} dist\left(x_h^i, M_j\left(x_h^i\right)\right)^{-1}}, \tag{8}$$

where $dist(a, b)$ denotes the Euclidean distance from a to b. The weighted mean of x_k^i in class $j(M_j\left(x_k^i\right))$ can be computed as

$$M_j\left(x_k^i\right) = \sum_{l=1}^{n_j} \omega_{kl}^{i,j} x_l^j, \tag{9}$$

where

$$\omega_{kl}^{i,j} = \frac{dist\left(x_k^i, x_l^j\right)^{-1}}{\sum_{h=1}^{n_j} dist\left(x_k^i, x_h^j\right)^{-1}}, \tag{10}$$

where x_l^j represents the lth sample in class j, and n_j is the number of sample of class j.

Subsequently, the nonparametric within-class scatter matrix ($\mathbf{S}_W^{NW}$) of NWFE in the original space $\mathbb{R}^m$ can be computed as

$$\mathbf{S}_W^{NW} = \sum_{i=1}^{C} \sum_{k=1}^{n_i} \frac{\lambda_k^{i,i}}{n_i} \left(x_k^i - M_i\left(x_k^i\right)\right)\left(x_k^i - M_i\left(x_k^i\right)\right)^T, \tag{11}$$

where the scatter matrix weight ($\lambda_k^{i,i}$) is defined as follows:

$$\lambda_k^{i,i} = \frac{dist\left(x_k^i, M_i\left(x_k^i\right)\right)^{-1}}{\sum_{h=1}^{n_i} dist\left(x_h^i, M_i\left(x_h^i\right)\right)^{-1}}. \tag{12}$$

The weighted mean of x_k^i in class i ($M_i\left(x_k^i\right)$) can be computed as

$$M_i\left(x_k^i\right) = \sum_{\substack{l=1 \\ l\neq k}}^{n_i} \omega_{kl}^{i,i} x_l^i, \tag{13}$$

where

$$\omega_{kl}^{i,i} = \frac{dist\left(x_k^i, x_l^i\right)^{-1}}{\sum_{\substack{h=1 \\ h\neq k}}^{n_i} dist\left(x_k^i, x_h^i\right)^{-1}}, \tag{14}$$

where x_l^i represents the lth sample in class i.

Finally, the reduced n-dimensional features are the first n eigenvectors with largest n eigenvalues of the following matrix:

$$\left(\mathbf{S}_W^{NW}\right)^{-1} \mathbf{S}_B^{NW}. \tag{15}$$

Then, we can obtain the transformation matrix ($\mathbf{S}$) based on the first n eigenvectors for reducing the original normalized feature vectors ($\mathbf{f}_k^n \in \mathbb{R}^m$) to the reduced feature vectors ($\mathbf{f}_k^r \in \mathbb{R}^n$) as follows:

$$\mathbf{f}_k^r = \mathbf{S}^T \mathbf{f}_k^n. \tag{16}$$

2) PRINCIPAL COMPONENT ANALYSIS

The PCA is utilized to find the significant feature vectors from the original normalized features in a projected space. the PCA utilizes a transformation matrix ($\mathbf{s}$) to transform the original normalized feature vectors in a m-dimensional space ($\mathbf{f}_K^N \in r^M$) into the reduced feature vectors in a n-dimensional space ($\mathbf{f}_K^R \in r^N$). firstly, the mean ($\mathbf{M}_N$) of the original normalized feature vectors and the covariance matrix ($\mathbf{c}_N$) are calculated as follows.

$$\mathbf{m}_n = \frac{1}{N} \sum_{k=1}^{N} \mathbf{f}_k^n, \tag{17}$$

$$\mathbf{C}_n = \frac{1}{N} \sum_{k=1}^{N} \left(\mathbf{f}_k^n - \mathbf{m}_n\right)\left(\mathbf{f}_k^n - \mathbf{m}_n\right)^T, \tag{18}$$

where N is the number of samples of the daily or sport activities. Then, we can choose the first n eigenvectors which are sorted according to their corresponding eigenvalue $\boldsymbol{\lambda}_k$ in descending order for construct the transformation matrix ($\mathbf{S}$).

$$\boldsymbol{\lambda}_k \mathbf{e}_k = \mathbf{C}_n \mathbf{e}_k, \tag{19}$$

$$\mathbf{S} = \{\mathbf{e}_k\}_{k=1}^n, \tag{20}$$

where $\boldsymbol{\lambda}_k$ is the eigenvalue associated with the eigenvector $\mathbf{e}_k$. Finally, we can obtain the reduced feature vectors ($\mathbf{f}_k^{\mathbf{r}} \in \mathbb{R}^n$) from the original normalized feature vectors ($\mathbf{f}_k^n \in \mathbb{R}^m$) via (16).

G. LS-SVM RECOGNIZER

After the feature reduction procedure, the reduced motion features can be used as inputs for a least squares support vector machine (LS-SVM) recognizer. The LS-SVM recognizer can divide the human daily activities into 1) walking (D1), 2) running (D2), 3) upstairs (D3), 4) downstairs (D4), 5) stand up and squat down (D5), 6) drinking (D6), 7) scrubbing (D7), 8) standing (D8), 9) sitting (D9), and 10) lying (D10), respectively. In addition, the LS-SVM recognizer can divide the sport activities into 1) table tennis (S1), 2) tennis (S2), 3) badminton (S3), 4) golf (S4), 5) pitching baseball (S5), 6) batting baseball (S6), 7) shooting basketball (S7), 8) volleyball (S8), 9) dribbling basketball (S9), 10) running (S10), and 11) bicycling (S11), respectively.

The LS-SVM is a binary classifier that utilizes a nonlinear mapping to transform the training data to a higher-dimensional space, wherein it can be well-separated by a separating hyperplane. Assume there are N data points in a training set, $\left\{\mathbf{x}_j, y_j\right\}_{j=1}^N$, where $\mathbf{x}_j = [x_{j1}, \ldots, x_{jn}] \in \mathbb{R}^n$ is the jth input feature vector (n is the number of dimensions of the reduced features obtained by the NWFE+PCA feature reduction method) and $y_j \in \{-1, 1\}$ is the jth output label. According to the structural risk minimization (SRM) principle of statistical learning theory, the risk bound of the LS-SVM is minimized by solving the following optimization problem:

$$\begin{aligned} &\min_{\mathbf{w},b,e} J\left(\mathbf{w}, b, e\right) = \frac{1}{2}\mathbf{w}^T\mathbf{w} + \frac{\gamma}{2}\sum_{j=1}^{N} e_j^2, \\ &\text{subject to : } y_j\left[\mathbf{w}^T\phi\left(\mathbf{x}_j\right) + b\right] = 1 - e_j, \quad j = 1, \ldots, N. \end{aligned} \tag{21}$$

The Lagrange method is used to solve this problem as follows:

$$\begin{aligned} &L\left(\mathbf{w}, b, e; \alpha\right) y_j \\ &\quad = J\left(\mathbf{w}, b, e\right) \\ &\qquad - \sum_{j=1}^{N} \alpha_j \left\{y_j\left[\mathbf{w}^T\phi\left(\mathbf{x}_j\right) + b\right] - 1 + e_j\right\}, \end{aligned} \tag{22}$$

where α_i are Lagrange multipliers, b is a real constant, and $\phi(\cdot)$ is a nonlinear mapping function to map the input space onto a higher dimensional space. Then, the equation can be solved by the Karush-Kuhn-Tucker (KKT) conditions and Mercer's Theorem [30]. More detailed information for the LS-SVM can be found in [30]–[32]. In this study, we use the LS-SVMs with one-against-one strategy to classify participants' daily and sport activities [31]. For classifying the target daily and sport activities in this study, the one-against-one method constructs $C(C-1)/2$ binary classifiers, where a max-wins voting strategy is utilized if C classes need to be classified. If the output of each LS-SVM classifier is one of the two classes, then the assigned class is increased by one vote. Finally, the classification result is represented as the class with largest votes. In this study, the output of the recognizer is represented as the label of the ten types of daily activities (i.e., walking (D1), running (D2),

upstairs (D3), downstairs (D4), stand up and squat down (D5), drinking (D6), scrubbing (D7), standing (D8), sitting (D9), and lying (D10) are labeled as '1', '2', '3', '4', '5', '6', '7', '8', '9', and '10') for the daily activity recognition task. On the other hand, for the sport activity recognition task, the output of the recognizer is represented as the label of the eleven types of sport activities (i.e., table tennis (S1), tennis (S2), badminton (S3), golf (S4), pitching baseball (S5), batting baseball (S6), shooting basketball (S7), volleyball (S8), dribbling basketball (S9), running (S10), and bicycling (S11) are labeled as '1', '2', '3', '4', '5', '6', '7', '8', '9', '10', and '11').

IV. EXPERIMENTAL RESULTS AND DISCUSSION

Our experiments were performed on a PC running Microsoft Windows 10 operating system with an Intel® Core Processor i5-4460 and 8-GB RAM. The recognition results recognized by the proposed activity recognition algorithm were compared to the video observation which was regarded as the criterion measure. In addition, we evaluated the recognition performances of the recognition schemes by the 2-fold, 5-fold, 10-fold, and leave-one-subject-out (LOSO) cross-validation strategies to investigate the robustness of our proposed algorithm. To evaluate the performances of the proposed recognition schemes, the measures of correct classification rate (*CCR*), accuracy (*Acc*), specificity (*Sp*), and sensitivity (*Se*) were utilized and defined as follows:

$$CCR(\%) = \frac{\sum_{i=1}^{C} TP_i}{TP + TN + FP + FN} \times 100, \quad (23)$$

$$Acc(\%) = \frac{TP + TN}{TP + TN + FP + FN} \times 100, \quad (24)$$

$$S_p(\%) = \frac{TN}{TN + FP} \times 100, \quad (25)$$

$$S_e(\%) = \frac{TP}{TP + FN} \times 100, \quad (26)$$

where *TP* is true positive, *TN* is true negative, *FP* is false positive, and *FN* is false negative. The *CCR* is used to evaluate the overall classification performance, where *C* is the number of classes.

A. HUMAN DAILY ACTIVITY RECOGNITION

In this experiment, each participant was invited to mount the wearable inertial sensor network on their wrist and ankle and execute daily activities in a laboratory environment. Fig. 6 shows the motion signal generated from the downstairs. In this paper, we compared the recognition performances of the LS-SVM recognizer between the six feature reduction methods, such as PCA [33], LDA [33], NWFE, PCA+LDA [33], NWFE+PCA, and NWFE+LDA, once the optimal dimensions of each of the feature reduction schemes were estimated. The overall CCRs of the PCA+LS-SVM, LDA+LS-SVM, NWFE+LS-SVM, PCA+LDA+LS-SVM, NWFE+PCA+LS-SVM, and NWFE+LDA+LS-SVM were achieved 96.38%, 86.00%, 96.92%, 94.38%, 98.23%, and 92.15% by the 10-fold cross-validation. The optimal numbers of the feature dimension used with the LS-SVM recognizer were reduced from 252 to 38 for PCA, 9 for LDA, 34 for NWFE, 4 for PCA+LDA, 18 for NWFE+PCA, and 8 for NWFE+LDA, which were shown in Table 2. The average accuracy of the PCA+LS-SVM, LDA+LS-SVM, NWFE+LS-SVM, PCA+LDA+LS-SVM, NWFE+PCA+LS-SVM, and NWFE+LDA+LS-SVM were 99.28%, 97.20%, 99.38%, 98.88%, 99.65%, and 98.43% by the 10-fold cross-validation. The recognition performance comparisons of the proposed feature reduction methods with the LS-SVM recognizers by the 2-fold, 5-fold, 10-fold, and LOSO cross-validation strategies are summarized in Table 3. Obviously, these results demonstrate that the NWFE+PCA+LS-SVM scheme can obtain the best recognition performance in comparison to other recognition schemes for recognizing the human daily activities. In addition, when we use one feature reduction method for the LS-SVM recognizer, the NWFE outperforms the PCA and LDA. The CCRs obtained by the 2-fold, 5-fold, 10-fold, and LOSO cross-validation strategies using the proposed NWFE+PCA+LS-SVM scheme were 96.69%, 97.46%, 98.23%, and 82.85%, respectively, in which the optimal numbers of the feature dimension was chosen by

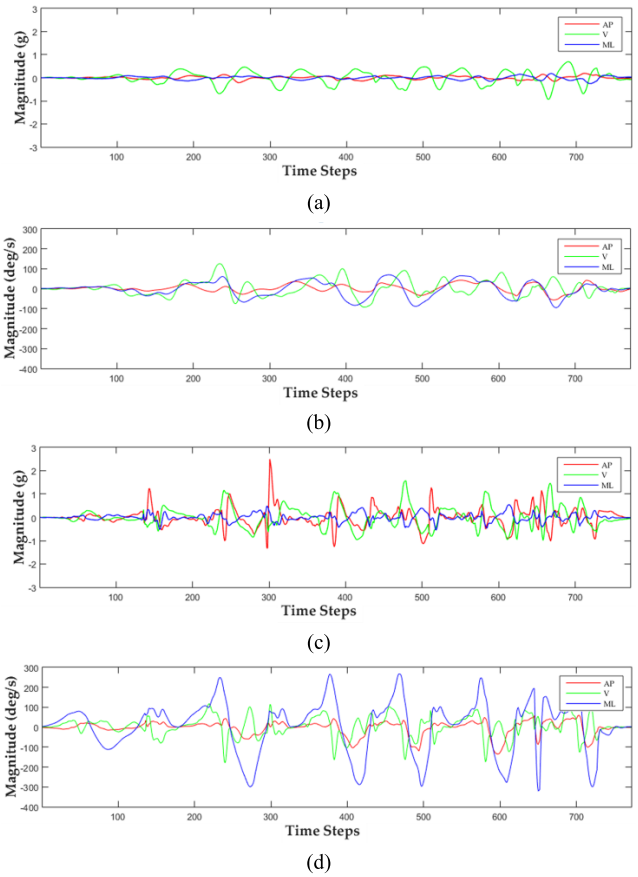

FIGURE 6. Motion signals generated from the downstairs activity. (a) Hand accelerations. (b) Hand angular velocities. (c) Foot accelerations. (d) Foot angular velocities.

TABLE 2. Recognition rates and reduced feature dimension for the proposed feature reduction methods with the LS-SVM recognizer by 10-fold cross-validation for human daily activity recognition.

Method	PCA	LDA	NWFE	PCA+LDA	NWFE+PCA	NWFE+LDA
CCR (%)	96.38	86.00	96.92	94.38	**98.23**	92.15
Acc (%)	99.28	97.20	99.38	98.88	**99.65**	98.43
Dimension	38	9	34	4 (171,4)	**18 (167,18)**	8 (129,8)

TABLE 3. Recognition performance comparisons of proposed feature reduction methods with LS-SVM recognizers by cross-validation in human daily activity recognition task.

K-fold / Reduction Method	2-fold				5-fold				10-fold				LOSO			
	Acc (%)	Sp (%)	Se (%)	CCR (%)	Acc (%)	Sp (%)	Se (%)	CCR (%)	Acc (%)	Sp (%)	Se (%)	CCR (%)	Acc (%)	Sp (%)	Se (%)	CCR (%)
PCA	99.00	99.44	95.00	95.00	99.05	99.47	95.23	95.23	99.28	99.60	96.38	96.38	94.92	97.18	74.62	74.62
LDA	96.20	97.89	81.00	81.00	97.18	98.44	85.92	85.92	97.20	98.44	86.00	86.00	93.43	96.35	67.15	67.15
NWFE	99.12	99.51	95.62	95.62	99.15	99.53	95.77	95.77	99.38	99.66	96.92	96.92	96.15	97.86	80.77	80.77
PCA+LDA	98.26	99.03	91.31	91.31	98.63	99.24	93.15	93.15	98.88	99.38	94.38	94.38	95.68	97.60	78.38	78.38
NWFE+PCA	**99.34**	**99.63**	**96.69**	**96.69**	**99.49**	**99.72**	**97.46**	**97.46**	**99.65**	**99.80**	**98.23**	**98.23**	**96.57**	**98.09**	**82.85**	**82.85**
NWFE+LDA	96.12	97.85	80.62	80.62	97.60	98.67	88.00	88.00	98.43	99.13	92.15	92.15	92.15	95.64	60.77	60.77

TABLE 4. Confusion matrix for human daily activity recognition using the NWFE+PCA+LS-SVM scheme verified by 10-fold cross-validation.

Activity \ Classified	D1	D2	D3	D4	D5	D6	D7	D8	D9	D10
D1	124	0	0	5	0	0	0	1	0	0
D2	2	127	1	0	0	0	0	0	0	0
D3	0	1	122	7	0	0	0	0	0	0
D4	2	0	4	124	0	0	0	0	0	0
D5	0	0	0	0	130	0	0	0	0	0
D6	0	0	0	0	0	130	0	0	0	0
D7	0	0	0	0	0	0	130	0	0	0
D8	0	0	0	0	0	0	0	130	0	0
D9	0	0	0	0	0	0	0	0	130	0
D10	0	0	0	0	0	0	0	0	0	130

the NWFE+PCA for the LS-SVM recognizer, i.e. 8 for 2-fold cross-validation, 66 for 5-fold cross-validation, 18 for 10-fold cross-validation, and 20 for LOSO cross-validation. The confusion matrix of the human daily activity recognition using the NWFE+PCA+LS-SVM scheme verified by the 10-fold cross-validation strategy is shown in Table 4. In terms of the runtime of the training processes, the NWFE+PCA+LS-SVM scheme spent 109 s, 197 s, 354 s, and 461 s by the 2-fold, 5-fold, 10-fold, and LOSO cross-validation strategies, respectively. Furthermore, the runtime of the test process was 1.66 s.

Additionally, from Table 4, we can fine that the misclassification occurred at walking, upstairs, and downstairs. The reason is that these three activities have identical characteristic features which are regular and periodic hand swing and foot-based motions. Obviously, from Figs. 6, 7, and 8, the hand accelerations of these three activities are similar and periodic, while the hand angular velocities of the walking and upstairs motions are similar. On the other hand, the foot accelerations of these three activities are also similar to each other.

B. SPORT ACTIVITY RECOGNITION

In the sport activity recognition, each participant was invited to mount the wearable inertial sensor network on their wrist and ankle and execute the eleven types of sport activities in a laboratory environment. Fig. 9 shows the motion signal generated from the bicycling. The overall CCRs of the PCA+LS-SVM, LDA+LS-SVM, NWFE+LS-SVM, PCA+LDA+LS-SVM, NWFE+PCA+LS-SVM, and NWFE+LDA+LS-SVM were achieved 97.82%, 73.91%, 99.36%, 97.09%, 99.55%, and 90.18% by the 10-fold cross-validation. The optimal numbers of the feature dimension used with the LS-SVM recognizers were reduced from 252 to 12 for PCA, 10 for LDA, 13 for NWFE, 10 for PCA+LDA, 50 for NWFE+PCA, and 4 for NWFE+LDA, which were shown in Table 5. The average accuracy of the PCA+LS-SVM, LDA+LS-SVM, NWFE+LS-SVM, PCA+LDA+LS-SVM, NWFE+PCA+LS-SVM, and NWFE+LDA+LS-SVM were 99.60%, 95.26%, 99.88%, 99.48%, 99.92%, and 98.22% by the 10-fold cross-validation. The recognition performance comparisons of the proposed feature reduction methods with the LS-SVM recognizers by the 2-fold, 5-fold, 10-fold, and LOSO cross-validation strategies are summarized in Table 6. Obviously, these results demonstrate that the proposed NWFE+PCA+LS-SVM scheme outperforms other recognition schemes for recognizing the sport activities. In addition, the NWFE feature reduction method can obtain better recognition

TABLE 5. Recognition rates and reduced feature dimension for the proposed feature reduction methods with the LS-SVM recognizer by 10-fold cross-validation for sport activity recognition.

Method	PCA	LDA	NWFE	PCA+LDA	NWFE+PCA	NWFE+LDA
CCR (%)	97.82	73.91	99.36	97.09	**99.55**	90.18
Acc (%)	99.60	95.26	99.88	99.48	**99.92**	98.22
Dimension	12	10	13	10 (11,10)	**50 (138,50)**	4 (10,4)

TABLE 6. Recognition performance comparisons of proposed feature reduction methods with LS-SVM recognizers by cross-validation in sport activity recognition task.

K-fold / Reduction Method	2-fold				5-fold				10-fold				LOSO			
	Acc (%)	Sp (%)	Se (%)	CCR (%)	Acc (%)	Sp (%)	Se (%)	CCR (%)	Acc (%)	Sp (%)	Se (%)	CCR (%)	Acc (%)	Sp (%)	Se (%)	CCR (%)
PCA	99.46	98.89	97.00	97.00	99.55	98.94	97.55	97.55	99.60	98.97	97.82	97.82	95.80	96.74	75.55	75.55
LDA	94.13	95.95	67.73	67.73	94.60	96.20	70.18	70.18	95.26	96.57	73.91	73.91	93.74	95.70	65.18	65.18
NWFE	99.29	98.80	96.09	96.09	99.83	99.09	99.09	99.09	99.88	99.12	99.36	99.36	99.38	98.84	96.55	96.55
PCA+LDA	99.38	98.84	96.55	96.55	99.45	98.88	96.91	96.91	99.48	98.91	97.09	97.09	91.67	94.84	51.00	51.00
NWFE+PCA	**99.87**	**99.10**	**99.27**	**99.27**	**99.88**	**99.11**	**99.36**	**99.36**	**99.92**	**99.13**	**99.55**	**99.55**	**99.20**	**98.73**	**95.45**	**95.45**
NWFE+LDA	95.29	96.81	74.09	74.09	97.49	97.93	86.18	86.18	98.22	98.28	90.18	90.18	92.88	95.64	59.82	59.82

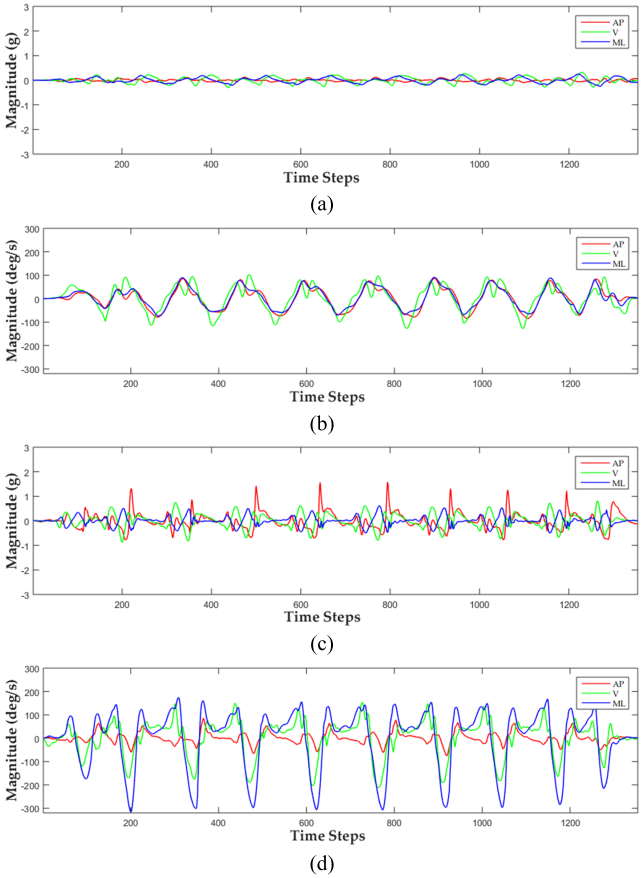

FIGURE 7. Motion signals generated from the walking activity. (a) Hand accelerations. (b) Hand angular velocities. (c) Foot accelerations. (d) Foot angular velocities.

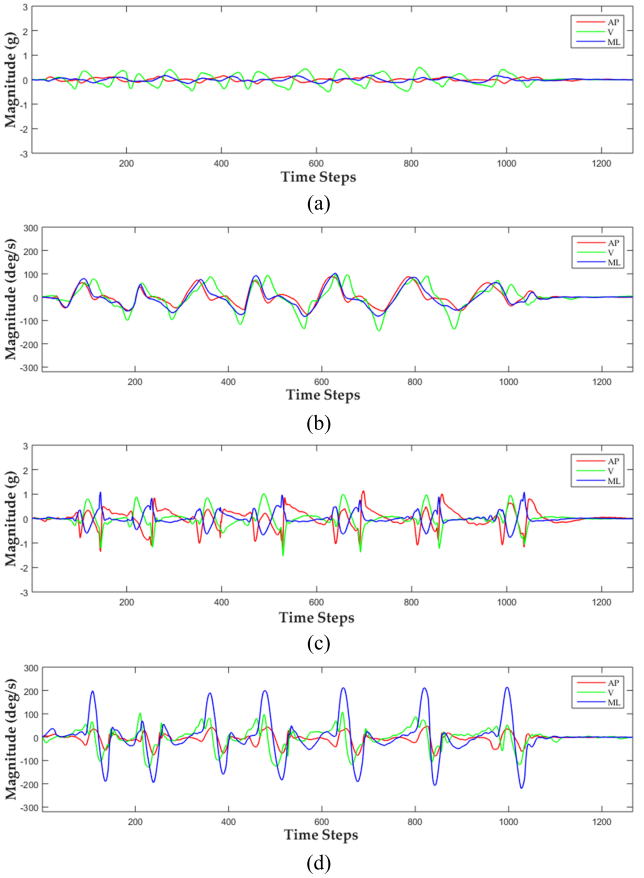

FIGURE 8. Motion signals generated from the upstairs activity. (a) Hand accelerations. (b) Hand angular velocities. (c) Foot accelerations. (d) Foot angular velocities.

performance than the PCA and LDA methods for the LS-SVM recognizer. The CCRs obtained by the 2-fold, 5-fold, 10-fold, and LOSO cross-validation strategies using the proposed NWFE+PCA+LS-SVM scheme were 99.27%, 99.36%, 99.55%, and 95.45%, respectively, in which the optimal numbers of the feature dimension was chosen by the NWFE+PCA for the LS-SVM recognizer, i.e. 52 for 2-fold cross-validation, 55 for 5-fold cross-validation, 50 for 10-fold cross-validation, and 53 for LOSO cross-validation. The confusion matrix of the sport activity recognition using

TABLE 7. Confusion matrix for sport activity recognition using the NWFE+PCA+LS-SVM scheme verified by 10-fold cross-validation.

Activity \ Classified	S1	S2	S3	S4	S5	S6	S7	S8	S9	S10	S11
S1	99	0	0	0	0	0	1	0	0	0	0
S2	0	100	0	0	0	0	0	0	0	0	0
S3	0	0	99	0	0	0	1	0	0	0	0
S4	0	0	0	100	0	0	0	0	0	0	0
S5	1	0	0	1	98	0	0	0	0	0	0
S6	0	1	0	0	0	99	0	0	0	0	0
S7	0	0	0	0	0	0	100	0	0	0	0
S8	0	0	0	0	0	0	0	100	0	0	0
S9	0	0	0	0	0	0	0	0	100	0	0
S10	0	0	0	0	0	0	0	0	0	100	0
S11	0	0	0	0	0	0	0	0	0	0	100

TABLE 8. Recognition performance comparisons of the proposed scheme with some existing schemes for human daily activity recognition.

Reference	Sensor	Placement	No. of Activity	No. of Feature	Feature selection/reduction	Classifier	Acc (%)	CCR (%)
Proposed method	Accelerometer, Gyroscope	Wrist, Ankle	10	252	NWFE+PCA	LS-SVM	99.65 (10-fold)	98.23 (10-fold)
[13]	Accelerometer	Waist	6	113	--	Majority voting model	95.90 (holdout)	--
[14]	Accelerometer, Gyroscope, Magnetometer	Chest, Thigh, Ankle	12	168	Wrapper approach based on random forest	k-NN	99.25 (10-fold)	--
[17]	Accelerometer, Barometer	Pocket, Holding	7	66	LS-SVM based SFS	LS-SVM	90.70	--
[16]	Accelerometer, Gyroscope	Body	6	559	FW	Naïve bayes	90.10 (5-fold)	--
[15]	Accelerometer, Temperature sensor, Altimeter	Wrist	9	63	Clamping technique	SVM	90.23 (10-fold)	--
[29]	Accelerometer	Wrist, Ankle, Chest	12	117	CFS	Rotation forest	98.00	--
[34]	Accelerometer, Gyroscope, Pressure sensor	Wrist, Ankle, Chest	16	131	ReliefF	k-NN	95.06	--
[18]	Accelerometer	Thigh	6	27	KDA	ELM	99.81	--
[20]	Accelerometer	Wrist	8	24	CPCA+SVC	FNN	--	95.24 (LOSO)
[19]	Accelerometer, Gyroscope, Magnetometer	Wrist, Knee, Chest	19	1170	PCA	Bayesian decision making	--	99.20 (10-fold)

TABLE 9. Recognition performance comparisons of the proposed scheme with some existing schemes for sport activity recognition.

Reference	Sensor	Placement	No. of Activity	No. of Feature	Feature selection/reduction	Classifier	Acc (%)	CCR (%)
Proposed method	Accelerometer, Gyroscope	Wrist, Ankle	11	252	NWFE+PCA	LS-SVM	99.92 (10-fold)	99.55 (10-fold)
[5]	Accelerometer, GPS	Wrist, Hip	9	7	--	Custom decision tree+ANN	89.00 (12-fold)	--
[6]	Accelerometer	Wrist	8	11	--	Logistic regression/ANN	85.00	--

the NWFE+PCA+LS-SVM scheme verified by the 10-fold cross-validation strategy is shown in Table 7. In terms of the runtime of the training processes, the NWFE+PCA+LS-SVM scheme spent 85 s, 154 s, 286 s, and 310 s by the 2-fold, 5-fold, 10-fold, and LOSO cross-validation strategies, respectively. Furthermore, the runtime of the test process was 1.71 s.

C. DISCUSSION

In this section, we compared the recognition performance of the proposed NWFE+PCA+LS-SVM scheme for human daily activity recognition with those of other schemes simultaneously utilizing different feature reduction methods and classifiers presented in the literature. We selected 10 existing activity classification schemes for comparison with our proposed scheme. The performance comparisons of our proposed scheme and 10 existing schemes for the human daily activity classification task are summarized in Table 8. The recognition results compares with the results reported in [13], [14], [17], [16], [15], [29], [34], and [18] whose average daily activity recognition accuracy are 95.90%, 99.25%, 90.70%, 90.10%, 90.23%, 98.00%, 95.06%, and 99.81%.

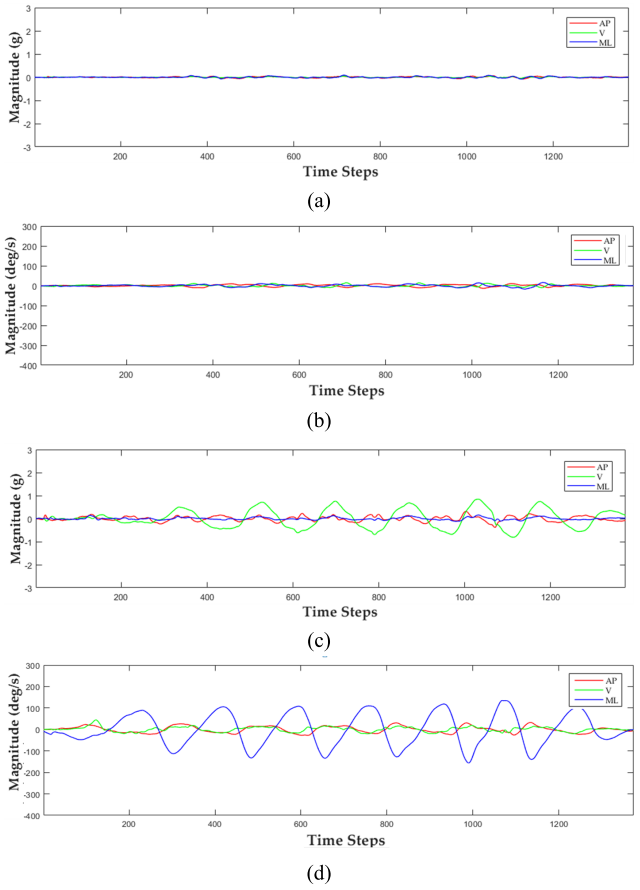

FIGURE 9. Motion signals generated from the bicycling activity. (a) Hand accelerations. (b) Hand angular velocities. (c) Foot accelerations. (d) Foot angular velocities.

Furthermore, the CCR of the proposed NWFE+PCA+LS-SVM scheme also compares with the results appeared in [19] and [20] whose CCRs are 95.24% and 99.20%. Hence, the experimental results show that the proposed wearable inertial sensor network with the activity recognition algorithm is effective to provide an accurate recognition rate in the daily activity recognition task.

On the other hand, 2 existing sport classification schemes are selected for comparison with our proposed scheme. The performance comparisons of our proposed scheme and 2 existing schemes for the sport activity recognition task are summarized in Table 9. The overall accuracy of the proposed NWFE+PCA+LS-SVM scheme was better than that of the hybrid classifier combining the custom decision tree and ANN [5] and the logistic regression (LR) or ANN [6] by more than 10.92% and 14.92%, respectively. Therefore, the results indicate that the proposed NWFE+PCA+LS-SVM scheme is the best combination for the sport activity recognition task. Note that, the abovementioned studies utilized various machine learning and feature selection/reduction methods to recognize numerous daily and sport activities with high accuracy; however, the performance of them would be affected by their individual datasets and number of daily and sport activities.

However, one of the limitations of this paper is that the proposed method has been evaluated on exemplar samples of human daily and sport activities that were conducted in a laboratory environment. In addition, the resources consumption in data transmission and processing for the proposed wearable network is high. In future studies, we intend to evaluate the proposed system in recognizing the motion signals measured by the inertial sensors in a free-living environment and reduce the sampling rate of the sensors for reducing the resources consumption of the proposed wearable network. Moreover, we will minimize the size of the wearable inertial sensing devices with improved wear comfortability.

V. CONCLUSIONS

In this paper, we present a wearable inertial sensor network and its associated activity recognition algorithm consisting of the NWFE+PCA feature reduction method and LS-SVM recognizer for recognizing the 10 human daily activities and 11 sport activities, respectively. The activity recognition algorithm is composed of motion signal acquisition, signal preprocessing, dynamic human motion detection, signal normalization, feature extraction, feature normalization, NWFE-PCA-based feature reduction, and LS-SVM recognizer. A total of 252 time- and frequency-domain features extracted from the accelerations and angular velocities generated from the hand and foot motions are used to provide distinguishing information for the daily and sport activity recognition tasks. Further, the 252-dimensional features are reduced to 18 and 50 new features by the NWFE+PCA feature reduction method to reduce the computational time and improving the recognition rates for the daily and sport activity recognition, respectively. The overall CCRs of 98.23% and 99.55% by the 10-fold cross-validation strategy for 10 daily activity classes and 11 sport activity classes, respectively, can be achieved by using the proposed NWFE+PCA+LS-SVM recognition scheme. Based on the abovementioned experimental results, the effectiveness of the proposed NWFE+PCA+LS-SVM scheme has been successfully validated. We believe that the proposed wearable inertial sensor network and its associated activity recognition algorithm can be regarded as an effective method for inertial-sensing-based human daily and sport activity recognition tasks.

REFERENCES

[1] M. Cornacchia, K. Ozcan, Y. Zheng, and S. Velipasalar, "A survey on activity detection and classification using wearable sensors," *IEEE Sensors J.*, vol. 17, no. 2, pp. 386–403, Jan. 2017.

[2] M. Seiffert, F. Holstein, R. Schlosser, and J. Schiller, "Next generation cooperative wearables: Generalized activity assessment computed fully distributed within a wireless body area network," *IEEE Access*, vol. 5, pp. 16793–16807, 2017.

[3] Y. Chen and C. Shen, "Performance analysis of smartphone-sensor behavior for human activity recognition," *IEEE Access*, vol. 5, pp. 3095–3110, 2017.

[4] M. Janidarmian, A. Roshan-Fekr, K. Radecka, and Z. Zilic, "A comprehensive analysis on wearable acceleration sensors in human activity recognition," *Sensors*, vol. 17, no. 3, p. 529, 2017.

[5] M. Ermers, J. Pärkkä, J. Mäntyjärvi, and I. Korhonen, "Detection of daily activities and sports with wearable sensors in controlled and uncontrolled conditions," *IEEE Trans. Inf. Technol. Biomed.*, vol. 12, no. 1, pp. 20–26, Jan. 2008.

[6] J. Margarito, R. Helaoui, A. M. Bianchi, F. Sartor, and A. G. Bonomi, "User-independent recognition of sports activities from a single wrist-worn accelerometer: A template-matching-based approach," *IEEE Trans. Biomed. Eng.*, vol. 63, no. 4, pp. 788–796, Apr. 2016.

[7] Y.-L. Hsu, J.-S. Wang, and C.-W. Chang, "A wearable inertial pedestrian navigation system with quaternion-based extended Kalman filter for pedestrian localization," *IEEE Sensors J.*, vol. 17, no. 10, pp. 3193–3206, May 2017.

[8] Y.-L. Hsu *et al.*, "Design and implementation of a smart home system using multisensor data fusion technology," *Sensors*, vol. 17, no. 7, p. 1631, 2017.

[9] M. Ueda, H. Negoro, Y. Kurihara, and K. Watanabe, "Measurement of angular motion in golf swing by a local sensor at the grip end of a golf club," *IEEE Trans. Human-Mach. Syst.*, vol. 43, no. 4, pp. 398–404, Jul. 2013.

[10] S. A. Rawashdeh, D. A. Rafeldt, and T. L. Uhl, "Wearable IMU for shoulder injury prevention in overhead sports," *Sensors*, vol. 16, no. 11, p. 1847, 2016.

[11] L. Cantelli, G. Muscato, M. Nunnari, and D. Spina, "A joint-angle estimation method for industrial manipulators using inertial sensors," *IEEE/ASME Trans. Mechatron.*, vol. 20, no. 5, pp. 2486–2495, Oct. 2015.

[12] J.-S. Wang, Y.-L. Hsu, and J.-N. Liu, "An inertial-measurement-unit-based pen with a trajectory reconstruction algorithm and its applications," *IEEE Trans. Ind. Electron.*, vol. 57, no. 10, pp. 3508–3521, Oct. 2010.

[13] I. C. Gyllensten and A. G. Bonomi, "Identifying types of physical activity with a single accelerometer: Evaluating laboratory-trained algorithms in daily life," *IEEE Trans. Biomed. Eng.*, vol. 58, no. 9, pp. 2656–2663, Sep. 2011.

[14] F. Attal, S. Mohammed, M, Dedabrishvili, F. Chamroukhi, L. Oukhellou, and Y. Amirat, "Physical human activity recognition using wearable sensors," *Sensors*, vol. 15, no. 12, pp. 31314–31338, 2015.

[15] S. Chernbumroong, S. Cang, A. Atkins, and H. Yu, "Elderly activities recognition and classification for applications in assisted living," *Expert Syst. Appl.*, vol. 40, no. 5, pp. 1662–1674, Apr. 2013.

[16] A. Wang, G. Chen, J. Yang, S. Zhao, and C.-Y. Chang, "A comparative study on human activity recognition using inertial sensors in a smartphone," *IEEE Sensors J.*, vol. 16, no. 11, pp. 4566–4578, Jun. 2016.

[17] F. Gu, A. Kealy, K. Khoshelham, and J. Shang, "User-independent motion state recognition using smartphone sensors," *Sensors*, vol. 15, no. 12, pp. 30636–30652, 2015.

[18] W. Xiao and Y. Lu, "Daily human physical activity recognition based on kernel discriminant analysis and extreme learning machine," *Math. Problems Eng.*, vol. 2015, no. 1, pp. 1–8, 2015.

[19] K. Altun, B. Barshan, and O. Tunçel, "Comparative study on classifying human activities with miniature inertial and magnetic sensors," *Pattern Recognit.*, vol. 43, no. 10, pp. 3605–3620, Oct. 2010.

[20] J.-Y. Yang, J.-S. Wang, and Y.-P. Chen, "Using acceleration measurements for activity recognition: An effective learning algorithm for constructing neural classifiers," *Pattern Recognit. Lett.*, vol. 29, no. 16, pp. 2213–2220, Dec. 2008.

[21] A. M. Khan, A. Tufail, A. M. Khattak, and T. H. Laine, "Activity recognition on smartphones via sensor-fusion and KDA-Based SVMs," *Int. J. Distrib. Sensor Netw.*, vol. 10, pp. 1–14, May 2014.

[22] Y.-P. Chen, J.-Y. Yang, S.-N. Liou, G.-Y. Lee, and J.-S. Wang, "Online classifier construction algorithm for human activity detection using a tri-axial accelerometer," *Appl. Math. Comput.*, vol. 205, no. 2, pp. 849–860, 2008.

[23] M. Elhoushi, J. Georgy, A. Noureldin, and M. J. Korenberg, "A survey on approaches of motion mode recognition using sensors," *IEEE Trans. Intell. Transp. Syst.*, vol. 18, no. 7, pp. 1662–1686, Jul. 2016.

[24] B.-C. Kuo and D. A. Landgrebe, "Nonparametric weighted feature extraction for classification," *IEEE Trans. Geosci. Remote Sens.*, vol. 42, no. 5, pp. 1096–1105, May 2004.

[25] B. C. Kuo, C. H. Li, and J. M. Yang, "Kernel nonparametric weighted feature extraction for hyperspectral image classification," *IEEE Trans. Geosci. Remote Sens.*, vol. 47, no. 4, pp. 1139–1155, Apr. 2009.

[26] H.-C. Chang, Y.-L. Hsu, S.-C. Yang, J.-C. Lin, and Z.-H. Wu, "A wearable inertial measurement system with complementary filter for gait analysis of patients with stroke or Parkinson's disease," *IEEE Access*, vol. 4, pp. 8442–8453, 2017.

[27] J.-S. Wang and F.-C. Chuang, "An accelerometer-based digital pen with a trajectory recognition algorithm for handwritten digit and gesture recognition," *IEEE Trans. Ind. Electron.*, vol. 59, no. 7, pp. 2998–3007, Jul. 2012.

[28] D. M. Karantonis, M. R. Narayanan, M. Mathie, N. H. Lovell, and B. G. Celler, "Implementation of a real-time human movement classifier using a triaxial accelerometer for ambulatory monitoring," *IEEE Trans. Inf. Technol. Biomed.*, vol. 10, no. 1, pp. 156–167, Jan. 2006.

[29] M. Arif and A. Kattan, "Physical activities monitoring using wearable acceleration sensors attached to the body," *PLoS ONE*, vol. 10, no. 7, p. e0130851, 2015.

[30] J. A. K. Suykens and J. Vandewalle, "Least squares support vector machine classifiers," *Neural Process. Lett.*, vol. 9, no. 3, pp. 293–300, Jun. 1999.

[31] C.-W. Hsu and C.-J. Lin, "A comparison of methods for multiclass support vector machines," *IEEE Trans. Neural Netw.*, vol. 13, no. 2, pp. 415–425, Mar. 2002.

[32] B. Liu, Z. Hao, and E. C. C. Tsang, "Nesting one-against-one algorithm based on SVMs for pattern classification," *IEEE Trans. Neural Netw.*, vol. 19, no. 12, pp. 2044–2052, Dec. 2008.

[33] J.-W. Wang, W.-C. Chiang, Y.-L. Hsu, and Y.-T. C. Yang, "ECG arrhythmia classification using a probabilistic neural network with a feature reduction method," *Neurocomputing*, vol. 116, pp. 38–45, Sep. 2013.

[34] A. Moncada-Torres, K. Leuenberger, R. Gonzenbach, A. Luft, and R. Gassert, "Activity classification based on inertial and barometric pressure sensors at different anatomical locations," *Physiol. Meas.*, vol. 35, no. 7, pp. 1245–1263, 2014.

YU-LIANG HSU (M'17) received the B.S. degree in automatic control engineering from Feng Chia University, Taichung, Taiwan, in 2004, and the M.S. and Ph.D. degrees in electrical engineering from National Cheng Kung University, Tainan, Taiwan, in 2007 and 2011, respectively.

He is currently an Assistant Professor with the Department of Automatic Control Engineering, Feng Chia University. His research interests include computational intelligence, biomedical engineering, nonlinear system identification, and wearable intelligent technology.

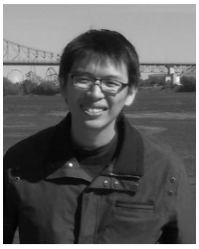

SHIH-CHIN YANG (S'10–M'12) was born in Kaohsiung, Taiwan. He received the M.S. degree from National Taiwan University, Taiwan, in 2007, and the Ph.D. degree from the University of Wisconsin-Madison, Madison, WI, USA, in 2011. From 2011 to 2015, he was a Research Engineer in Texas Instruments Motor Lab, Dallas, TX, USA. In 2015, he became a Faculty Member with National Taiwan University, where he is currently an Associate Professor responsible for the investigation of motor drive and PWM control technology. His research interests include motor drive, power electronics, and control systems.

Dr. Yang received one conference prize paper award from the IEEE Industry Applications Society Industrial Drive Committee in 2011 and one presentation award from the IEEE Energy Conversion Congress and Exposition in 2016.

HSING-CHENG CHANG received the B.S. and M.S. degrees in physics from Tamkang University, Taiwan, in 1978 and 1980, respectively, and the M.S. and Ph.D. degrees in electrical and computer engineering from the University of Cincinnati, Cincinnati, OH, USA, in 1991 and 1994, respectively.

He is currently a Professor with the Department of Automatic Control Engineering, Feng Chia University, Taiwan. His research interests include microsensors and microactuators, circuit design, automation technology, and engineering education.

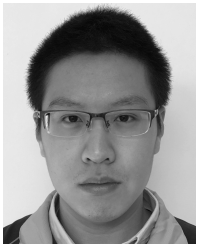

HUNG-CHE LAI received the B.S. and M.S. degrees in automatic control engineering from Feng Chia University, Taichung, Taiwan, in 2015 and 2017. His research interests include signal processing and wearable devices.